ANALYSIS OF FLOOD FLOWS IN MOUNTAIN STREAMS WITH BOULDERS AND ROCKS BY USING NON-HYDROSTATIC QUASI THREE-DIMENSIONAL MODEL (Q3D-FEBS)

SHOJI FUKUOKA [1], YOSHIHARU TAKEMURA [2] & JYUNKI OHNO [3]

[1,2] Research and Development Initiative, Chuo University, Tokyo, Japan,
takemura@tamacc.chuo-u.ac.jp

[3] Graduate School of Science and Engineering, Chuo University, Tokyo, Japan,
a12.fd7b@g.chuo-u.ac.jp

ABSTRACT

The value of the Manning's roughness coefficients (= n) for mountain streams varies considerably in time and space due to the complex riverbed geometry including boulders and rocks. It reduces the reliability of the flood flow analysis in mountain streams. In this paper, the 2017 flood of the Takiyama River is analyzed by using 2D flow model and Q3D-FEBS based on observed water surface profiles for the reach where the detailed riverbed geometry including the shapes of boulders and rocks was measured. The results show that the value of n can be almost invariably determined from the flood flows and channel geometry by taking account of the three-dimensional flow velocities and non-hydrostatic pressure distributions around the boulders and rocks by using Q3D-FEBS. This makes it possible to estimate flood discharge hydrographs and flow structures from the reliable flood flow analysis in mountain streams.

Keywords: Mountain streams, boulders, flood flows, water surface profiles, Q3D-FEBS

1   INTRODUCTION

Mountain streams are characterized by steep bed gradients and complex riverbed geometry including boulders and rocks. The flood flow analysis in the mountain streams is necessary for many aspects, such as prediction of flood water levels and velocities, estimation of channel discharge capacity and formation of stable habitats. Flow resistance in the mountain streams have been studied by many researchers (e.g. Bathurst 1985, Ferguson 2007, David 2010 and Asano 2016). However, the values of the roughness coefficients (e.g. the Manning's roughness coefficient and the Darcy-Weisbach friction factor) calculated in these studies vary considerably not only sites, but also with time dependent water depths and discharges of floods. Most of the studies used discharges as input data. However, it should be taken into account that the discharge measurement in the mountain streams is less accurate than the water level measurement because of the violent flood flows (e.g. Bathurst 1990).

Fukuoka proposed a comprehensive method of flood flow analysis using time series data of observed water surface profiles. The Fukuoka's method enables reliable flood flow analysis by numerically solving the flow equations in such a way as to coincide with the observed water surface profiles that can be accurately observed at multiple points during floods (Fukuoka 2017a and 2017b). In lowland rivers where the riverbed materials are composed of sand and gravel, flood flow characteristics such as discharge hydrographs and velocity distributions can be estimated with reasonable accuracy from two-dimensional flood flow analysis based on the Fukuoka's method. Then, the values of the Manning's roughness coefficient n can be well predicted from the riverbed materials and they are almost invariant with time in many cases. On the other hand, in the mountain streams, the values of n calculated by the Fukuoka's method are considerably large compared to the riverbed materials and they vary with time (Tsukamoto et al., 2016 and Ohno et al., 2018a). This is probably because the flow resistance arising from complex riverbed geometry of the mountain streams that cannot be measured by normal topographic surveys. If these can be considered in flood flow analysis suitable for mountain streams, we can reasonably determine the values of n and reliable flood flow analysis will be possible based on the Fukuoka's method in the mountain streams, too.

Recently, we developed a new non-hydrostatic quasi three-dimensional model (Q3D-FEBS) that introduced the flow equations on boundary surfaces (the free surface and the bottom surface) (Ohno et al., 2018b). Q3D-FEBS can calculate the three-dimensional velocity and pressure distributions due to the complex riverbed geometry of the mountain streams with high computational efficiency compared to 3D flow model. This paper presents the applicability of Q3D-FEBS for estimating the flood discharge hydrographs and flow structures

in the mountain streams based on the Fukuoka's method in comparison with 2D flow model, while targeting flood flows of the reach where the detailed riverbed geometry including the shapes of boulders and rocks was measured.

2   GORVERNING EQUATIONS OF Q3D-FEBS

The definition sketch of Q3D-FEBS is shown in Figure 1. We define the bottom surface z_b slightly above the bed surface z_0. A vertical coordinate is given as $\eta = (z_s - z)/h$ and approximates vertical distributions of the horizontal velocities by the third-order polynomial.

$$u_i = \Delta u_i(12\eta^3 - 12\eta^2 + 1) + \delta u_i(-4\eta^3 + 3\eta^2) + U_i \qquad [1]$$

Where, $i = 1, 2$ ($x_1 = x$, $x_2 = y$), u_i: velocity in i direction, U_i: depth-average velocity in i direction, u_{si}: water surface velocity in i direction, u_{bi}: bottom surface velocity in i direction, $\Delta u_i = u_{si} - U_i$, $\delta u_i = u_{si} - u_{bi}$, z_s: water level, h: water depth. The boundary conditions used in the derivation of Eq. [1] are as follows.

$$u_i = u_{si}, \quad \partial u_i/\partial z = 0 \quad at \quad \eta = 0 \ (z = z_s) \qquad [2]$$

$$u_i = u_{bi} \quad at \quad \eta = 1 \ (z = z_b) \qquad [3]$$

$$\int_0^1 u_i \, d\eta \ \left(= \frac{1}{h}\int_{z_b}^{z_s} u_i \, dz\right) = U_i \qquad [4]$$
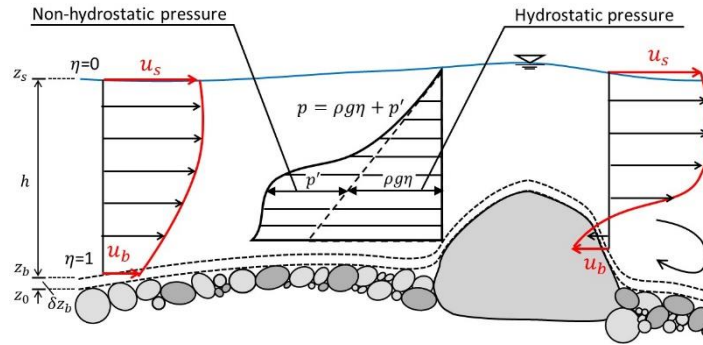

Figure 1. Definition sketch of Q3D-FEBS.

Q3D-FEBS solves the equations of motion on a free surface ($\eta = 0$) and a bottom surface ($\eta = 1$) in addition to the depth-integral flow equations shown by Eq. [5] and Eq. [6] to calculate the unknown quantities of Eq. [1].

$$\frac{\partial h}{\partial t} + \frac{\partial U_i h}{\partial x_i} = 0 \qquad [5]$$

$$\frac{\partial U_i h}{\partial t} + \frac{\partial U_j U_i h}{\partial x_j} = -gh\frac{\partial z_s}{\partial x_i} - \frac{1}{\rho}\frac{\partial h\overline{p'}}{\partial x_i} - \frac{p'_b}{\rho}\frac{\partial z_b}{\partial x_i} - \frac{\partial h\overline{u'_i u'_j}}{\partial x_j} + \frac{\partial}{\partial x_j}\overline{\nu_t}h\left(\frac{\partial U_i}{\partial x_j} + \frac{\partial U_j}{\partial x_i}\right) - \hat{S}\frac{\hat{\tau}_{bi}}{\rho} \qquad [6]$$

Where, ρ: density of water, $u'_i = u_i$- U_i, g: acceleration of gravity, p': non-hydrostatic pressure, ν_t: eddy viscosity, $\hat{\tau}_{bi}$: bottom shear stress in i direction, $\hat{S} = \sqrt{1 + (\partial z_b/\partial x_i)^2}$. Overbar "–" represents a depth-averaged value. The form resistance of boulders and rocks can be calculated from the third term of Eq. [6] that represents the non-hydrostatic pressure received from riverbeds. The non-hydrostatic pressure in Eq. [6] are calculated by Eq. [7] derived from the depth-integral equation of motion in the vertical direction.

$$\frac{p'_b}{\rho} = U_i h\frac{\partial W}{\partial x_i} + \hat{S}\frac{\hat{\tau}_{bz}}{\rho}, \frac{\overline{p'}}{\rho} = \frac{1}{2}\frac{p'_b}{\rho} + \frac{U_i h}{12}\frac{\partial(w_s - w_b)}{\partial x_i} \qquad [7]$$

Where, W: depth-average velocity in the vertical direction, w_s: water surface velocity in the vertical direction, w_b: bottom surface velocity in the vertical direction. W is obtained from Eq. [1] and the equation of continuity.

$$W = \frac{1}{2}\frac{\partial(z_s + z_b)}{\partial t} + \frac{1}{2}U_i\frac{\partial(z_s + z_b)}{\partial x_i} + \frac{1}{h}\frac{\partial}{\partial x_i}h^2\left(\frac{\delta u_i}{20} + \frac{\Delta u_i}{10}\right) \qquad [8]$$

w_s and w_b are given from the kinematic boundary conditions at the water surface and the bottom surface.

$$w_s = \frac{\partial z_s}{\partial t} + u_{si}\frac{\partial z_s}{\partial x_i}, \quad w_b = \frac{\partial z_b}{\partial t} + u_{bi}\frac{\partial z_b}{\partial x_i} \qquad [9]$$

Eq. [10] and Eq. [11] are the equations of motion on the water surface ($\eta = 0$) and the bottom surface ($\eta = 1$).

$$\frac{\partial u_{si}}{\partial t} + u_{sj}\frac{\partial u_{si}}{\partial x_j} = -g\frac{\partial z_s}{\partial x_i} + \frac{1}{\rho}\frac{\partial p'}{\partial z}\bigg|_s\frac{\partial z_s}{\partial x_i} + \frac{v_{ts}}{\rho}\frac{\partial^2 u_i}{\partial z^2}\bigg|_s \tag{10}$$

$$\frac{\partial u_{bi}}{\partial t} + u_{bj}\frac{\partial u_{bi}}{\partial x_j} = -g\frac{\partial z_s}{\partial x_i} - \frac{1}{\rho}\frac{\partial p'_b}{\partial x_i} + \frac{1}{\rho}\frac{\partial p'}{\partial z}\bigg|_b\frac{\partial z_b}{\partial x_i} + \frac{\partial}{\partial x_j}v_{tb}\left(\frac{\partial u_{bi}}{\partial x_j} + \frac{\partial u_{bj}}{\partial x_i}\right) + \frac{\hat{S}}{\rho}\frac{\hat{\tau}_{bi} - \hat{\tau}_{0i}}{\delta z_b} \tag{11}$$

Where, $\hat{\tau}_{0i}$: bed shear stress in i direction, $\delta z_b = c_{zb}h$, c_{zb} = 0.03. The shear stress and pressure at the water surface are assumed 0. The gradient of the non-hydrostatic pressure in the vertical direction at the water surface and the bottom surface are calculated from Eq. [12] derived from the equations of motion in the vertical direction on the water surface and the bottom surface.

$$\frac{1}{\rho}\frac{\partial p'}{\partial z}\bigg|_s = -u_{si}\frac{\partial w_s}{\partial x_i}, \quad \frac{1}{\rho}\frac{\partial p'}{\partial z}\bigg|_b = -u_{bi}\frac{\partial w_b}{\partial x_i} \tag{12}$$

The bottom shear stress and the bed shear stress are evaluated by Eq. [13] and Eq. [14], respectively.

$$\hat{\tau}_{0i} = \rho c_b^2 u_{bi}|\boldsymbol{u_b}|, \quad \hat{\tau}_{0z} = \rho c_b^2 w_b|\boldsymbol{u_b}| \tag{13}$$

$$\hat{\tau}_{bi} = v_{tb}\frac{\partial u_i}{\partial z}\bigg|_b, \quad \hat{\tau}_{bz} = \frac{\hat{\tau}_{0z}}{c_{zb} + 1} \tag{14}$$

$$c_b = \frac{C_0}{1 - 2C_0/\kappa}\sqrt{1 + c_{zb}}, \quad C_0 = \sqrt{\frac{gn^2}{h^{1/3}}} \tag{15}$$

Where, $\partial^2 u_i/\partial z^2|_s = (-24\Delta u_i + 6\delta u_i)/h^2$, $\partial u_i/\partial x|_s = (-12\Delta u_i + 6\delta u_i)/h$, n: the Manning's roughness coefficient, κ = 0.41. The eddy viscosities are assumed constant along a vertical direction ($\overline{v_t} = v_{ts} = v_{tb}$) and given as follows.

$$\overline{v_t} = \frac{1}{6}\kappa u_* h\frac{1}{\sqrt{1 + c_{zb}}} \tag{16}$$

3   USEFULNESS OF Q3D-FEBS FOR FLOOD FLOW ANALYSIS IN MOUNTAIN STREAMS WITH BOULDERS AND ROCKS

3.1   Studied reach and flood

The Takiyama River is located in Hiroshima Prefecture, Japan. The studied reach is 4.58 km to 6.3 km (the Kurotaki observation station) upstream from the Nukui Dam (catchment area of 253km^2) in the Takiyama River (see Figure 2). The average riverbed gradient is about 0.02. The detailed riverbed geometry including the shapes of boulders and rocks was measured by aerial photography survey using a drone. In addition, pressure type water level gauges have been installed at the point of ◯ in Figure 2. They were fastened to very large rocks as shown in Figure 3.

Figure 4 shows aerial photographs of Area 1, Area 2 and Area 3 shown in Figure 2. Boulders and rocks of 1 to 3 m in height are distributed on the riverbed. Figure 5 shows the inflow and outflow discharge hydrographs of the Nukui Dam and the water level hydrograph in the reservoir observed during the 2017 flood in the Takiyama River. The 2017 flood is a record-breaking flood after the dam construction. The water level gauges installed at 4.9 km and 5.8 km were unfortunately washed away during the flood, but we could obtain water level data at other points. We performed flood flow analysis with target to Jul. 2:00 to Jul. 17:00 in Figure 5.
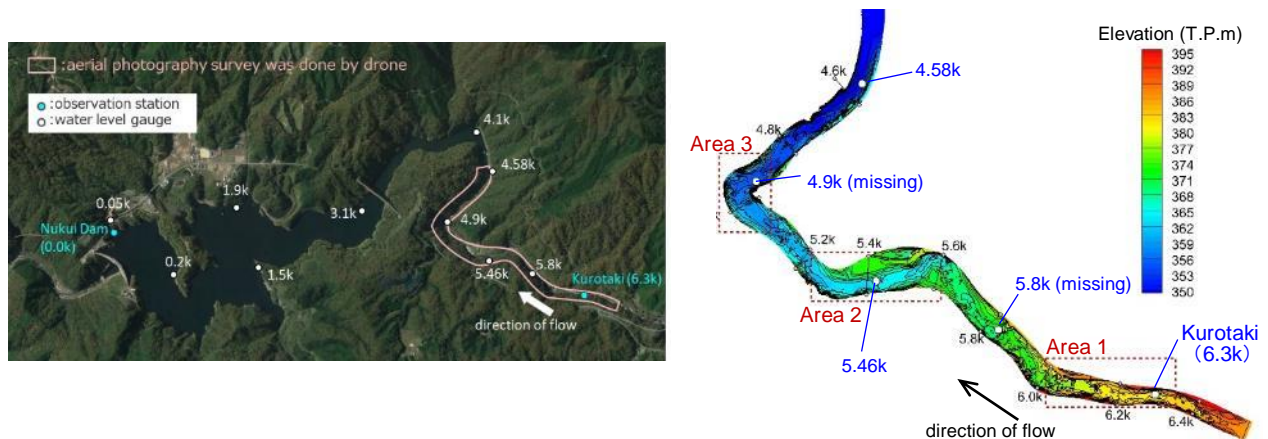

Figure 2. Location and observation system of the studied reach.

(a) 4.9 km

(b) 5.46 km

Figure 3. Water level gauges at 4.9 km and 5.46 km points.

(a) Area 1

(b) Area 2

(c) Area 3

Figure 4. Aerial photographs of Area 1, Area 2 and Area 3 shown in Figure 2.
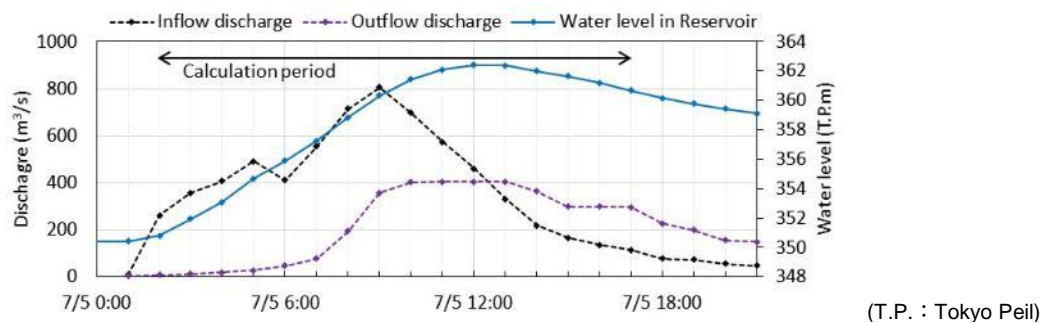

(T.P.：Tokyo Peil)

Figure 5. Inflow and outflow discharge hydrographs of the Nukui Dam and water level hydrograph in the reservoir observed during the 2017 flood of the Takiyama River.

3.2 Computational grid

Riverbed geometry of the studied reach was measured at 30 cm intervals by the aerial photographic survey. Figure 6 shows the cross-sectional shapes at 5.4 km point based on the normal topographic survey at 200 m intervals and the aerial photography survey. The normal water level and the maximum water level for the 2017 flood at 5.46 km are shown in Figure 6. The riverbed elevations of the aerial photographic survey tend to be higher than that of the normal topographic survey at a location lower than the normal water level. On the other hand, riverbed elevations of these surveys show good agreements at a location above the normal water level. This indicates that the aerial photographic survey may overestimate the riverbed elevation under the water surface. However, the shapes of boulders and rocks projecting from the water surface can be correctly measured by the aerial photographic survey.
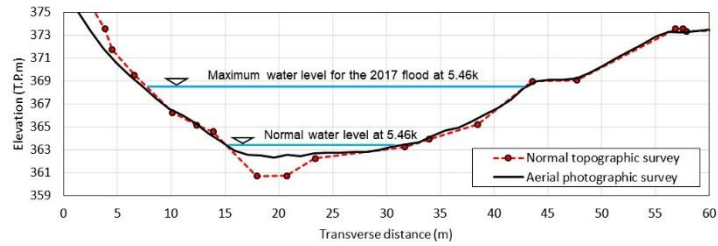
Figure 6. Cross-sectional shapes by normal topographic survey and aerial photographic survey at 5.4 km point.

Q3D-FEBS can consider both skin-friction and form drag of boulders and rocks by incorporating their shapes into the computational grid. Therefore, computational grid size is an important factor to estimate the flow resistance. We used computational grid size of 1 m with reference to our previous study (Ohno et al., 2018b). The riverbed elevations of the computational grid were given by averaging the aerial photographic survey data within each grid cell. Figure 7 shows comparison of the 3D riverbed elevation contours by the aerial photographic survey and the computational grid. The computational grid can almost reproduce the shapes of boulders and rocks of several meters in size, which are considered to be the main source of flow resistance in the studied reach. The flow resistance due to the small roughness which cannot represent the shape by the computational grid is evaluated by the Manning's roughness coefficient n.
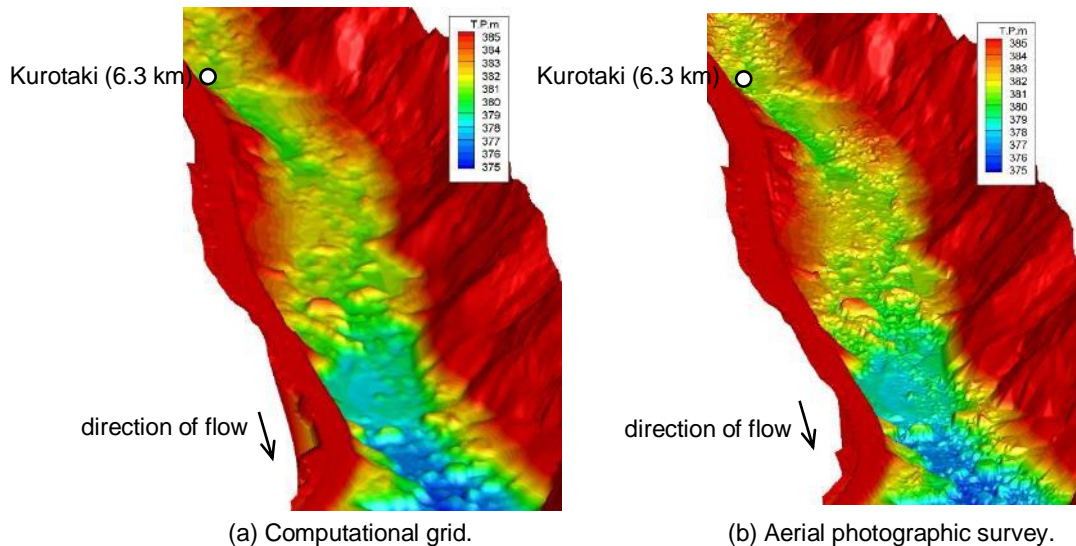

(a) Computational grid.   (b) Aerial photographic survey.

Figure 7. 3D riverbed elevation contours by aerial photographic survey and computational grid.

3.3   Usefulness of Q3D-FEBS for flood flow analysis in mountain streams with boulders and rocks

At first, we analyzed the 2017 flood in the Takiyama River based on the time series data of the observed water surface profiles in the studied reach by using following two calculation methods.

(1) Conventional 2D method: a computational grid is created from the normal topographic survey at 200 m intervals and 2D flow model is used for flood flow analysis.
(2) Present method: a computational grid is created in the manner described in 3.2 and Q3D-FEBS is used for flood flow analysis.

The boundary conditions at upstream and downstream ends are given by the observed water level hydrographs at the Kurotaki observation station (6.3 km) and at 4.58 km point, respectively. Figure 8 shows the comparison of the observed and calculated water surface profiles in the rising period of the 2017 flood. Figure 9 shows comparison of calculated discharge hydrographs at the Kurotaki observation station (6.3km) and the inflow discharge hydrograph of the Nukui Dam. The calculations results can almost explain the observation results. In Figure 8 (b), the water levels calculated by the present method tends to be slightly higher than the observed data at 5.46 km point. It is probably because that the riverbed elevations of the computational grid around 5.46 km point may contain errors as pointed out in 3.2 since there are few boulders and rocks projecting from the water surface (see Figure 4 (b)).
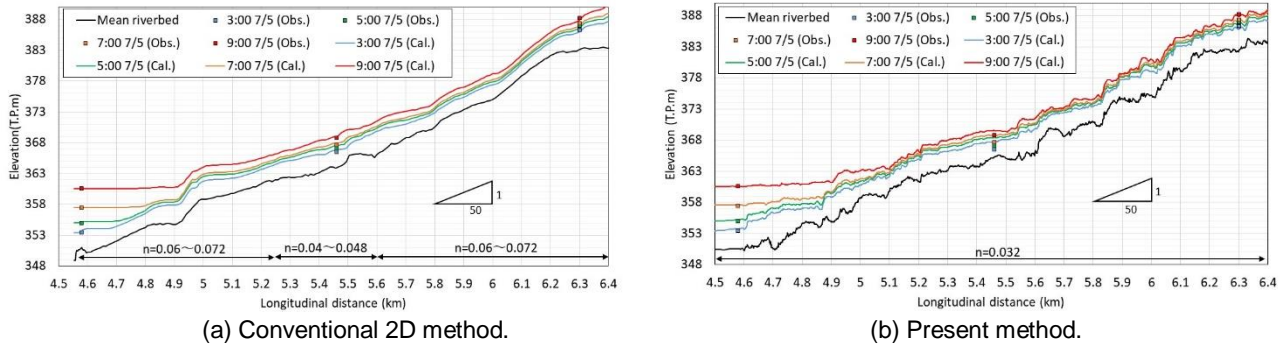
(a) Conventional 2D method.　　　　　　　　(b) Present method.

Figure 8. Observed and calculated water surface profiles in rising period of the 2017 flood.
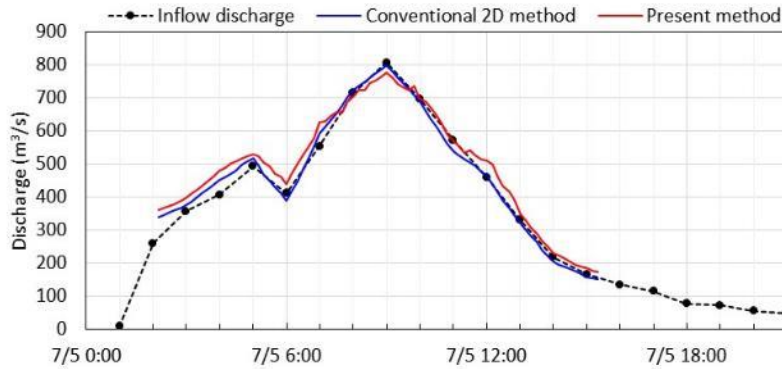

Figure 9. Calculated discharge hydrographs at the Kurotaki observation station (6.3 km) and inflow discharge hydrograph of the Nukui Dam for the 2017 flood.

The values of the Manning's roughness coefficient n calculated by the conventional 2D method and the present method are compared in Table 1. They are determined in a way as to explain the temporal changes in observed water surface profiles and the inflow discharge hydrograph of the Nukui Dam as mentioned above. In the conventional method, the values of n are in the range of 0.04 to 0.072, and it is necessary to change the values over time in order to coincide with observed water surface profiles. On the other hand, in the present method, n has a constant value of 0.032, which is a reasonable value from the engineering sense about mountain streams. It can be noticed that the water surface profiles calculated by the present method shown in Figure 8 (b) are clearly affected by the longitudinal mean riverbed profiles in comparison with the conventional 2D method (Figure 8 (a)). This indicates that observation errors of the mean riverbed elevations have influences on the calculated n values. In addition to this, as discussed on the following, the flow structures in the mountain streams are three-dimensional due to the influence of complex riverbed geometry including boulders and rocks. These are the reasons why the n value of the conventional method varies in time and space. Although such a problem remains, the most important fact is that the flood discharge hydrographs by the conventional 2D method as well as the present method can be calculated in a sense that the flood flow analysis based on the time series data of the observed water surface profiles as shown in Figure 8 and Figure 9 is performed.

Table 1. The Manning's roughness coefficient n calculated by the conventional 2D and present methods.

		2:00 – 6:00 7/5	6:00 – 9:00 7/5	9:00 – 12:00 7/5	12:00 – 15:00 7/5
Conventional method	6.4 – 5.6 km	0.06	0.06 → 0.072	0.072 → 0.06	0.06
	5.6 – 5.25 km	0.04	0.04 → 0.048	0.048 → 0.04	0.04
	5.25 – 4.5 km	0.06	0.06 → 0.072	0.072 → 0.06	0.06
Present method	6.4 – 4.5 km	0.032			

In the following, the applicability of 2D flow model and Q3D-FEBS to the estimation of flow structures in mountain streams is discussed. For this purpose, we analyze the 2017 flood by the following method.

(3) 2D method: a computational grid is created in the manner described in 3.2 and 2D flow model is used for flood flow analysis.

Figure 10 show the comparison of calculation results by the present method and the 2D method in the flood peak for the reach of 6.0 km to 6.2km where the boulders and rocks in several meters are densely distributed. Figure 11 and Figure 12 are calculated velocity distributions by the present method and the 2D method in A-A' and B-B' cross-sections shown in Figure 10 (a). In the surrounding of the large boulders and rocks seen in

Figure 10 (a), non-hydrostatic pressure head at the bottom is more than 1 m in absolute value and the velocity distributions become three-dimensionally complicated (see Figure 10 (b) and Figure 12). These three-dimensional effects cannot be considered in the 2D method. As a result, the calculated water levels and velocities vary extremely around the large boulders and rocks as shown in Figure 10 (c), (e) and Figure 11. On the other hand, the present method shows the plausible results as shown in Figure 10 (d), (f) and Figure 12. Especially, Figure 12 indicates the tendency that velocities near the riverbeds are reduced under the influence of the non-uniformly distributed boulders and rocks and the flow velocities near the water surface increase. This is consistent with the results reported in the previous study (Bathurst 1990). These results indicate that the flow structures in the mountain streams are three-dimensional due to the presence of large boulders and rocks. Therefore, the three-dimensional flow structures such as velocity distributions, local water levels and non-hydrostatic pressure distributions cannot be represented by 2D flow model even if the detailed geometry is taken into account. The three-dimensional flow structures in the mountain streams can be estimated by performing Q3D-FEBS based on the observed water surface profiles and the detailed riverbed geometry including the shapes of boulders and rocks. It will also extend the discussion on the sediment transport, riverbed variations, and formations of stable habitats in the mountain streams.
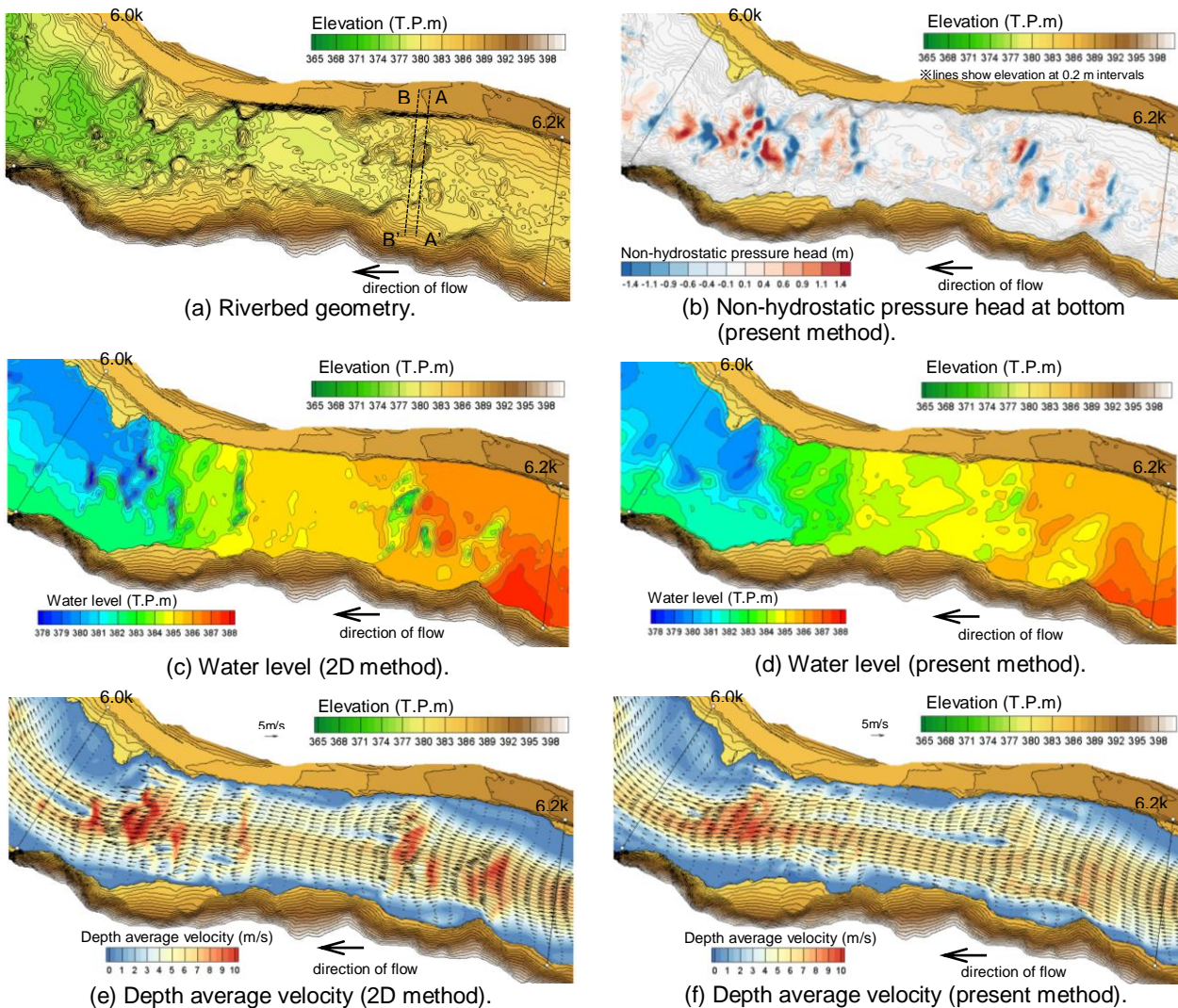

Figure 10. Calculation results of 2D method and present method in the 2017 flood peak for the reach of 6.0 km to 6.2km.
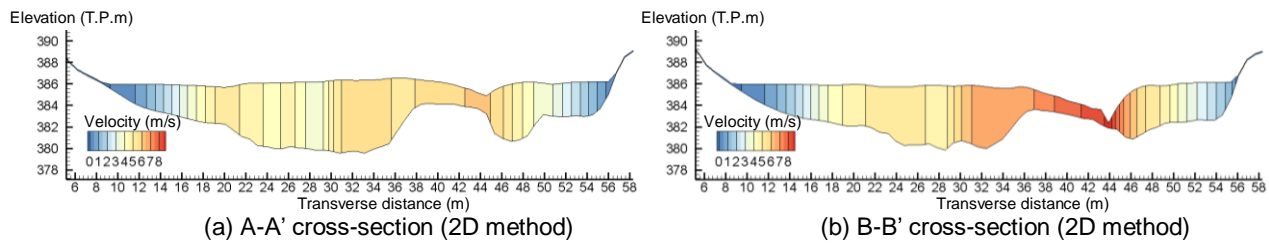
(a) A-A' cross-section (2D method) (b) B-B' cross-section (2D method)

Figure 11. Velocity distributions by 2D method in A-A' and B-B' cross-sections shown in Figure 10 (a).

(a) A-A' cross-section (present method) (b) B-B' cross-section (present method)
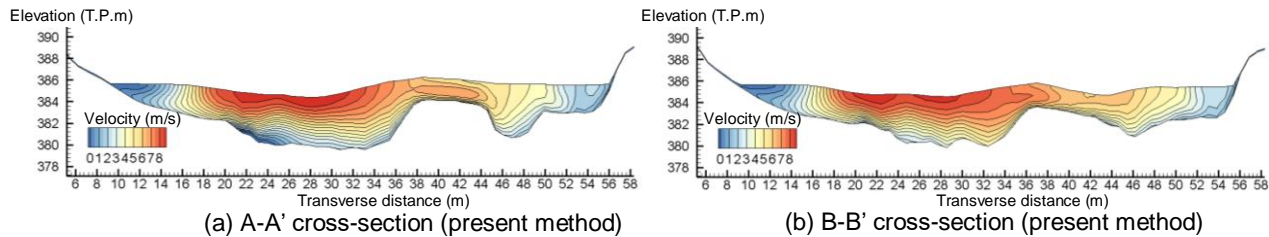
Figure 12. Velocity distributions by present method in A-A' and B-B' cross-sections shown in Figure 10 (a).

4   CONCLUSIONS

In this paper, the usefulness of Q3D-FEBS for the flood flow analysis based on the time series data of the observed water surface profiles for the mountain streams with boulders and rocks was investigated from the comparison with 2D flow model. Main conclusions are shown below.

1. Flood discharge hydrographs in the mountain streams can be approximately estimated by the conventional 2D method using the normal topographic survey at 200 m intervals if the flood flow analysis is performed based on the times series data of the observed water surface profiles. In this case, the Manning's roughness coefficient has considerably large values compared to the riverbed materials and the values vary with time.

2. Flow structures such as velocity distributions and local water levels in the mountain streams are three-dimensionally complicated due to the influence of the complex riverbed geometry including boulders and rocks and that cannot be represented by 2D flow model even if the detailed riverbed geometry is taken into account.

3. The flood discharge hydrographs and three-dimensional flow structures in the mountain streams can be estimated from the reliable flood flow analysis by using Q3D-FEBS, detailed riverbed geometry and the observed water surface profiles. Then the roughness coefficients can be determined reasonably from the flood flows and channel geometry.

REFERENCES

Asano, T. and Uchida, T. (2016). Detailed documentation of dynamic changes in flow depth and surface velocity during a large flood in a steep mountain stream. J*ournal of Hydrology*, 541, 127-135.

Bathurst J.C. (1985). Flow resistance estimation in mountain rivers. *Journal of Hydraulic Engineering*, 111(4), 625-643.

Bathurst, J.C. (1990). Tests of three discharge gauging techniques in mountain rivers. Hydrology of Mountainous Areas, IAHS, Wallingford, UK, 93–100.

David, G.C.L., Wohl, E., Yochum, S.E. and Bledsoe B.P. (2010). Controls on spatial variations in flow resistance along steep mountain streams. *Water Resources Research*, 46, W03513.

Ferguson, R. (2007). Flow resistance equations for gravel- and boulder-bed streams. *Water Resources Research*, 43, W05427.

Fukuoka, S. (2017a). Current significance of water level and discharge of river floods. *Annual Journal of Hydraulic Engineering*, JSCE, 61, I_355-I_360 (in Japanese).

Fukuoka, S. (2017b). Creating an idea of integrated river plan due to the use of widespread water surface profiles of floods in river basins. *Advances in River Engineering*, JSCE, 23, 251-256 (in Japanese).

Ohno, J., Fukuoka, S. and Tanabe, H. (2018a). On the discharge estimation method of flood flows in mountain streams based on multiple-water levels observation data. *Annual Journal of Hydraulic Engineering*, JSCE, 62, I_799-I_804 (in Japanese).

Ohno, J., Fukuoka, S., Takemura, Y. and Nigo, S., (2018b). Analsis of flood flows in mountain streams with boulders by using non-hydrostatic quasi-three dimensional model (Q3D-FEBS). Proceedings of the 32nd Symposium on Computational Fluid Dynamics, JSFM, C01-1 (in Japanese).

Tsukamoto, Y., Fukuoka, S. and Oyama, O. (2016). Study on the evaluation method of inflow and outflow discharges considering flood flow dynamics in the Kusaki Dam reservoir. *Advances in River Engineering*, JSCE, 22, 7-12 (in Japanese).